MOLECULAR AND CELLULAR BIOLOGY, Nov. 2009, p. 6046–6058 Vol. 29, No. 22
0270-7306/09/$12.00 doi:10.1128/MCB.00654-09

Muscle Lim Protein Interacts with Cofilin 2 and Regulates F-Actin Dynamics in Cardiac and Skeletal Muscle[▽]

Vasiliki Papalouka,[1] Demetrios A. Arvanitis,[1] Elizabeth Vafiadaki,[1] Manolis Mavroidis,[2] Stavroula A. Papadodima,[3] Chara A. Spiliopoulou,[3] Dimitrios T. Kremastinos,[4] Evangelia G. Kranias,[1,5] and Despina Sanoudou[1,6]*

Molecular Biology Division, Biomedical Research Foundation of the Academy of Athens, Athens, Greece[1]; Cell Biology Division, Biomedical Research Foundation of the Academy of Athens, Athens, Greece[2]; Department of Forensic Medicine and Toxicology, Medical School, National and Kapodistrian University of Athens, Athens, Greece[3]; Second Department of Cardiology, University of Athens, Attikon Hospital, Athens, Greece[4]; Department of Pharmacology and Cell Biophysics, College of Medicine, University of Cincinnati, Cincinnati, Ohio[5]; and Department of Pharmacology, Medical School, National and Kapodistrian University of Athens, Athens, Greece[6]

Received 20 May 2009/Returned for modification 12 June 2009/Accepted 4 August 2009

The muscle LIM protein (MLP) and cofilin 2 (CFL2) are important regulators of striated myocyte function. Mutations in the corresponding genes have been directly associated with severe human cardiac and skeletal myopathies, and aberrant expression patterns have often been observed in affected muscles. Herein, we have investigated whether MLP and CFL2 are involved in common molecular mechanisms, which would promote our understanding of disease pathogenesis. We have shown for the first time, using a range of biochemical and immunohistochemical methods, that MLP binds directly to CFL2 in human cardiac and skeletal muscles. The interaction involves the inter-LIM domain, amino acids 94 to 105, of MLP and the amino-terminal domain, amino acids 1 to 105, of CFL2, which includes part of the actin depolymerization domain. The MLP/CFL2 complex is stronger in moderately acidic (pH 6.8) environments and upon CFL2 phosphorylation, while it is independent of Ca^{2+} levels. This interaction has direct implications in actin cytoskeleton dynamics in regulating CFL2-dependent F-actin depolymerization, with maximal depolymerization enhancement at an MLP/CFL2 molecular ratio of 2:1. Deregulation of this interaction by intracellular pH variations, CFL2 phosphorylation, MLP or CFL2 gene mutations, or expression changes, as observed in a range of cardiac and skeletal myopathies, could impair F-actin depolymerization, leading to sarcomere dysfunction and disease.

The muscle LIM protein (MLP) has emerged as a critical player in striated muscle physiology and pathophysiology over recent years. MLP, encoded by the *CSRP3* (or *CRP3*) gene, is a member of the conserved LIM-only protein family since it contains two LIM functional zinc finger domains, and it is expressed exclusively in muscle cells. Specifically, in differentiating striated muscle cells, MLP localizes in the nucleus, promoting myogenic differentiation (8), while in adult muscle, it translocates to the cytoplasm and assumes an essential role in myocyte cytoarchitecture. Through its interactions with structural proteins, such as alpha-actinin, telethonin (T-cap), βI-spectrin, and N-RAP, MLP has been suggested to act as a scaffold protein for the basic contractile unit, the sarcomere, and the actin-based cytoskeleton (7, 9, 25, 27, 46, 73).

Mutations in *CSRP3* have been directly associated with dilated (DCM) and hypertrophic (HCM) cardiomyopathies (9, 31, 32, 46). HCM is the most common genetic myocardial disease, with a prevalence of 0.2% in adults, and the most frequent cause of sudden cardiac death in young individuals, while DCM is the third most common cause of heart failure (54, 55, 76). Genetic aberrations in MLP have been shown to lead to marked actin cytoskeleton disorganization and disrupted cardiac myofibrillar cytoarchitecture (9). Similar observations have been described for skeletal muscles, and HCM-*CSRP3* mutations have been associated with mild skeletal myopathy (9, 31). Various hypotheses, including an MLP role in mechanical stretch sensing or the mechanical stress response, have been formulated to link the molecular and histological observations with the clinical phenotype, but important information appears to still be missing.

At the expression level, significant changes in MLP have been observed in cardiac muscle following myocardial infarction, as well as in heart failure, and in the skeletal muscles in a number of neuromuscular disorders (13, 24, 40, 72, 81, 83, 84, 89). Interestingly, *CSRP3* was one of the only two consistently changed transcripts, among the hundreds of significant gene expression changes, across the skeletal muscles analyzed in a recent study of nemaline myopathy (NM), suggesting a strong association with the pathological phenotype (72). NM, a disease characterized by the formation of nemaline rods, which consist of aggregations of sarcomeric proteins such as α-actinin and filamentous actin within myocytes, is the most common nondystrophic congenital myopathy (71).

Although NM arises primarily from mutations in thin filament proteins; a novel mutation was recently discovered in the actin depolymerization protein cofilin 2 (CFL2) (3). CFL2 is a muscle-specific protein that belongs to the actin depolymerization factor (ADF)/cofilin family (65, 80). These proteins have a critical role in the regulation of actin filament dynamics by enhancing the turnover of actin filaments in a variety of cells

* Corresponding author. Mailing address: Molecular Biology Division, Biomedical Research Foundation of the Academy of Athens, Soranou Efesiou 4, Athens 115-27, Greece. Phone: 30-210-6597055. Fax: 30-210-6597545. E-mail: dsanoudo@enders.tch.harvard.edu.
▽ Published ahead of print on 14 September 2009.

(60, 63, 80). Despite a wealth of data related to the action of other cofilins, little is known about the function of CFL2 in muscle cells. Recently, decreased levels of CFL2 were associated with reduced depolymerization of actin filaments, causing their accumulation in nemaline rods (3). The association of both MLP and CFL2 with actin cytoskeleton aberrations and (cardio)myopathic phenotypes led us to hypothesize that there might be a link between the two proteins.

To examine this hypothesis, we performed a series of biochemical and subcellular localization experiments. Our results reveal the direct and specific interaction of MLP and CFL2, the intracellular parameters affecting this interaction, and its implications in actin depolymerization. Importantly, we show that the MLP/CFL2 stoichiometry plays a critical role in actin depolymerization in vitro. Therefore, perturbations in their interaction and activity, caused by either pathological mutations or expression changes, would be anticipated to directly affect actin dynamics and in this way the sarcomeric and actin cytoskeleton structure, ultimately resulting in myocyte dysfunction and muscle disease.

MATERIALS AND METHODS

Tissue specimens and protein preparation. Postmortem human cardiac and skeletal quadriceps muscle specimens were obtained from the Department of Forensics and Toxicology, Medical School, National and Kapodistrian University of Athens. Whole-protein extracts were prepared using Ultra-Turrax Tissuemizer (IKA-Werke GmbH & Co., Staufen, Germany) in ice-cold lysis buffer (10 mM $NaPO_4$, pH 7.2, 2 mM EDTA, 10 mM NaN_3, 120 mM NaCl, and 1% Nonidet P-40) supplemented with a mixture of protease inhibitors (Sigma-Aldrich Gmbh, Munich, Germany). The protein concentration and quality were determined using the Quant-iT protein assay kit (Invitrogen Corp., Eugene, OR) on a Qubit fluorometer (Invitrogen Corp., Eugene, OR) according to the manufacturer's instructions. The protein extracts were aliquoted and stored at −80°C. The research protocol was approved by the institutional ethics committee and conformed to the principles outlined in the Declaration of Helsinki (57).

Construction of recombinant proteins. In order to generate the human MLP and CFL2 constructs, total RNA was isolated from human postmortem nonfailing cardiac tissue using TRIzol (Invitrogen, Carlsbad, CA) according to the manufacturer's instruction. Reverse transcription was performed using Superscript II RNase H reverse transcriptase (Invitrogen), and the cDNA was then used as a template for PCR amplification. For the generation of full-length and deletion constructs of MLP, the PCR products were digested with EcoRI/SalI (Takara Bio, Otsu, Shiga, Japan) restriction enzymes and cloned into the pMAL-c2X vector (New England Biolabs, Beverly, MA). The following primer sets were used for amplification: 5′-ATC GGA ATT CGT CTT CAA GAT GCC AAA C-3′ and 5′-ATC GGT CGA CTC TGT GCA GGA TTA CTT G-3′ for maltose binding protein (MBP)-MLP (amino acids [aa] 1 to 195), 5′-ATG CGA ATT CAA ATG TGG AGC CTG TGA A-3′and 5′-ACT GGT CGA CGA CTG TTG GAA CTG CAG G-3′ for MBP-MLP-LIM1 (aa 9 to 94), 5′-ACG TGA ATT CAG CAA CCC TTC CAA ATT C-3′ and 5′-ACG TGT CGA CTG TTG TGT AAG GCC TCC A-3′ for MBP-MLP-LIM2 (aa 105 to 188), and 5′-ATG CGA ATT CCG CAG ATA TGG CCC CAA A-3′and 5′-ATC GGT CGA CGG ACT CTC CAA CTT CGC-3′ for MBP-MLP-inter-LIM (aa 64 to 117). For the generation of the CFL2 constructs, PCR products were digested with EcoRI/XhoI (Takara Bio, Otsu, Shiga, Japan) and subcloned into the pGEX-5X vector (Amersham Biosciences Europe). The primers for CFL2 amplification were as follows: 5′-ATG CGA ATT CAT GGC TTC TGG AGT TAC A-3′and 5′-ATG CCT CGA GTG GCA CTT GAC TGT CAT T-3′ for GST-CFL2 (aa 1 to 166), 5′-CCG TGA ATT CAC ATG GCT TCT GGA GTT-3′ and 5′-ACG TCT CGA GCA AGA TCT GCT TTG CTT C-3′ for GST-CFL2-A (aa 1 to 55), 5′-ACG TGA ATT CAA GTC ATC AAA GTT T-3′and 5′-ACG TCT CGA GCT ACT ACA TTG CCT C-3′ for GST-CFL2-B (aa 105 to 166), and 5′-ATG CGA ATT CAG ATC TTG GTG GGT GAC-3′ and 5′-ATG CCT CGA GAC TTT CAG GAG CCC A-3′ for GST-CFL2-C (aa 55 to 108). The sequences of all generated constructs were verified by automated sequencing (Macrogen, Seoul, South Korea). Glutathione *S*-transferase (GST) and MBP fusion proteins were expressed by induction with 0.5 mM isopropyl-β-D-thiogalactopyranoside for 4 h in the BL21 Star (Invitrogen) and library efficient DH5α (Invitrogen) *Escherichia coli* strains. The recombinant proteins were purified by affinity chromatography using glutathione Sepharose 4B beads (Amersham Biosciences) for GST fusion proteins or amylose resin beads for MBP fusion proteins (New England Biolabs), according to the manufacturer's instructions.

Pull-down assays. Human nonfailing cardiac and skeletal muscle tissue specimens were homogenized in 10 mM $NaPO_4$, pH 7.2, 2 mM EDTA, 10 mM NaN_3, 120 mM NaCl, and 1% (vol/vol) NP-40 supplemented with a mixture of protease inhibitors (Sigma-Aldrich). Equivalent amounts of recombinant GST and GST-CFL2 proteins bound to glutathione-Sepharose 4B resin were mixed with 0.5 mg of cardiac or skeletal homogenates. After 16 h of incubation at 4°C, the beads were washed three times with 10 mM $NaPO_4$, pH 7.2, 10 mM NaN_3, 120 mM NaCl, and 3.5% (vol/vol) Tween 20, analyzed by 10% sodium dodecyl sulfate-polyacrylamide gel electrophoresis (SDS-PAGE), and transferred to a nitrocellulose membrane. The membranes were probed with the polyclonal chicken anti-MLP antibody (1:700 dilution; AbCam, Cambridge, United Kingdom), washed in 50 mM Tris-HCl (pH 7.5), 150 mM NaCl, and 0.05% (vol/vol) Tween 20, and incubated with a peroxidase-conjugated rabbit anti-chicken secondary antibody (1:33,000 dilution; AbCam). Immunoreactive bands were visualized using electrogenerated chemiluminescence (ECL) reagents according to the manufacturer's protocol (Amersham Biosciences).

In vitro binding assay. In vitro binding assays were performed by mixing MBP-MLP protein bound to amylose resin matrices with equivalent amounts (5 μg) of recombinant GST-CFL2 and GST proteins in 50 μl binding buffer (50 mM Tris-HCl [pH 7.4], 120 mM NaCl, 10 mM NaN_3, 2 mM dithiothreitol, 0.5% Tween 20). Following a 16-h incubation at 4°C, the beads were washed three times with a solution containing 50 mM Tris-HCl (pH 7.4), 120 mM NaCl, 10 mM NaN_3, and 0.1% Tween 20. In a parallel set of experiments, 5 μg of recombinant MBP-MLP and MBP were allowed to interact with GST-CFL2 proteins attached to glutathione matrices, as described above. All samples were analyzed by 10% SDS-PAGE, transferred to a nitrocellulose membrane, and incubated with rabbit anti-GST (1:2,500 dilution; Amersham Biosciences Europe, Uppsala, Sweden) or rabbit anti-MBP (1:10,000 dilution; New England Biolabs, Beverly MA) antibodies, followed by peroxidase-conjugated goat anti-rabbit (1:33,000 dilution; Amersham Biosciences Europe) secondary antibody.

Blot overlay assays. The blot overlay assays were performed as previously described (10). Briefly, aliquots containing ~2.5 μg of affinity-purified GST, GST-CFL2-A (aa 1 to 55), GST-CFL2-B (aa 55 to 108), and GST-CFL2-C (aa 105 to 166) fusion proteins were separated by 10% SDS-PAGE and transferred to nitrocellulose membranes. Blocking of nonspecific sites on the membrane was performed in buffer A (50 mM Tris-HCl [pH 7.5], 150 mM NaCl, 0.05% [vol/vol] Tween 20, 2 mM dithiothreitol, 0.5% NP-40, 5% nonfat milk) for 16 h at 4°C. The samples were then incubated with 3 μg/ml MBP-MLP (aa 1 to 195) fusion protein in buffer A in the presence of 1 mM ATP for 5 h at 25°C. At the end of this incubation period, the blots were subjected to five 20-min washes in buffer C (50 mM Tris-HCl [pH 7.5], 150 mM NaCl, 0.05% [vol/vol] Tween 20, 2 mM dithiothreitol, 1% NP-40) at 25°C. Subsequently, the membranes were probed with anti-MBP for 2 h at 25°C, and the labeled bands were visualized using ECL reagents. In a set of parallel assays, 3 μg of affinity-purified MBP, MBP-MLP (aa 1 to 195), MBP-MLP-LIM1 (aa 9 to 94), MBP-MLP-LIM2 (aa 105 to 188), and MBP-MLP-inter-LIM (aa 64 to 117) fusion proteins were each subjected to 10% SDS-PAGE, transferred to nitrocellulose membranes, and allowed to interact with GST-CFL2 protein as described above.

Immunofluorescence staining. Human quadriceps muscle specimens were transversely sectioned at 10-μm thickness, placed on polysine-coated microscope slides (Sigma-Aldrich), and fixed in ice-cold methanol for 20 min. Slides were washed in phosphate-buffered saline (PBS) (1×) and permeabilized for 30 min at 25°C in PBS containing 0.1% (vol/vol) Triton X-100. After washing with PBS, the slides were blocked with PBS containing 1 mg/ml bovine serum albumin–10 mM NaN_3 for 1 h at 25°C. Primary antibodies, including chicken anti-MLP (1:333; AbCam), rabbit anti-CFL2 (1:400 dilution; Upstate, Millipore, MA), mouse anti-α-actinin (1:1,000; Sigma-Aldrich), or rhodamine-conjugated phalloidin (1:100 dilution; Invitrogen), were applied to the sections and were incubated for 2 h at 25°C. Following washes with 1× PBS, the samples were counterstained for 1 h with the appropriate secondary antibody: fluorescein isothiocyanate anti-chicken (1:400 dilution; AbCam), Alexa Fluor 488 anti-rabbit (1:400 dilution), or Alexa Fluor 488 anti-mouse (1:400 dilution; Invitrogen). Following washes with 1× PBS, the samples were mounted with Vectashield medium containing 4′,6-diamidino-2-phenylindole (Vector Laboratories, Burlingame, CA) and analyzed with a Leica confocal laser scanning microscope (TCS SP5, DMI6000; inverted with the acquisition software program LAS-AF).

pH dependence experiments. To study the effect of pH on the interaction of MLP with CFL2, in vitro binding assays were performed using a range of pH values. Equivalent amounts of MBP-MLP and MBP proteins bound to amylose

resin matrices were incubated with 5 μg of recombinant GST-CFL2 protein in 50 μl reaction buffer, containing 120 mM NaCl, 10 mM NaN_3, 2 mM dithiothreitol, 0.5% Tween 20, and 50 mM Tris-HCl with variable pH values (pH 6.8, pH 7.4, pH 8.0, and pH 8.4). After a 16-h incubation at 4°C, the samples were washed three times with 120 mM NaCl, 10 mM NaN_3, 0.1% Tween 20, and 50 mM Tris-HCl at various pH values as noted above and analyzed by 10% SDS-PAGE and immunoblotting. The quantification of the intensities of the bands of interest was performed using the Image J software program (version 1.33a).

Phosphorylation experiments. The effect of CFL2 phosphorylation on its interaction with MLP was studied through in vitro phosphorylation assays, using endogenous kinases of freshly prepared mouse cardiac protein extracts (19). Briefly, 5 μg of affinity-purified GST-CFL2 was incubated with the protein extracts in 3.1 mM ATP, 3 mM NaF, and 3 mM Na_3VO_4 at 25°C for 30 min. The samples were washed three times with wash buffer (15 mM NaF, 2 mM Na_3VO_4, 50 mM Tris-HCl [pH 7.5], 150 mM NaCl, 0.05% [vol/vol] Tween 20). The phosphorylation of GST-CFL2 was confirmed by Western blotting using rabbit polyclonal anti-CFL2 (1:600 dilution; Upstate, Millipore, MA) or rabbit polyclonal anti-phospho-CFL2 (P-CFL2) (1:500 dilution; Upstate) as the primary antibody. Blot overlay assays were performed on phosphorylated and unphosporylated forms of CFL2, as described above.

pCa dependence experiments. pCa is a measure of calcium ion (Ca^{2+}) concentration ($pCa = -\log[Ca^{2+}]$). To investigate the effect of calcium on the interaction of MLP with CFL2, blot overlay assays were performed as described above under different concentrations of Ca^{2+}. Specifically, consecutive dilutions of 10^{-5} M to 10^{-8} M $CaCl_2$ were added to the aforementioned buffer B.

Actin depolymerization assay. The Actin Polymerization Biochem kit (Cytoskeleton, Denver, CO) was used to investigate actin dynamics in vitro on a PerkinElmer LS 55 Fluorescence spectrometer (PerkinElmer Ltd., Bucks, United Kingdom). Briefly, pyrene-labeled F-actin was prepared by incubating 0.1 mg pyrene G-actin, diluted in G buffer (5 mM Tris-HCl [pH 8.0], 0.2 mM $CaCl_2$) with 10× actin polymerization buffer (0.25× final strength) (500 mM KCl, 20 mM $MgCl_2$, 10 mM ATP) at room temperature for 1 h. The solution of pyrene F-actin was transferred in Herazil quartz cuvettes with two polished windows (Hellma GmbH, Mullheim, Germany) and placed in the fluorometer. The depolymerization of pyrene F-actin was measured by fluorescence spectrometer counts at an excitation wavelength of 365 nm with emission at 407 nm within 30-s intervals. The optimal wavelengths were selected after a wavelength scan. A four-position automatic cuvette cell changer, including water thermostatting and stirring for each sample position, allowed the simultaneous, multiple time-dependent measurements of four samples. The F-actin depolymerization was performed in the presence/absence of GST-CFL2 or phosphorylated GST-CFL2 and MBP-MLP or MBP-MLP-inter-LIM at pH 8.0 or pH 6.8.

Coimmunoprecipitation experiments. The experiment was performed as previously described with minor modifications (48). Hearts from normal adult 129SV and desmin null mice ($Des^{-/-}$) (a kind gift from Y. Capetanaki) were flash-frozen in liquid nitrogen and homogenized in 100 μl of homogenization buffer (10 mM $NaPO_4$, pH 7.2, 2 mM EDTA, 10 mM NaN_3, 120 mM NaCl, 1% [vol/vol] NP-40) supplemented with a mixture of protease inhibitors (Sigma-Aldrich). Equal amounts of the protein extracts were precleared with 80 μl of protein A-Sepharose beads (Amersham Biosciences) for 3 h at 4°C. In parallel, 5 mg of anti-CFL2 antibodies were incubated with 100 μl of protein A beads for 3 h at 4°C. The precleared cardiac extracts were subsequently incubated with the CFL2 antibody bound to the protein A beads at 4°C for 16 h. A sample lacking the primary antibody was used as a negative control. The beads were washed three times with wash buffer (10 mM $NaPO_4$, pH 7.2, 10 mM NaN_3, 140 mM NaCl, 0.5% [vol/vol] NP-40, 0.5% [vol/vol] Tween 20) and analyzed by Western blotting using the MLP antibody (1:700 dilution; AbCam). Anti-β-actin (1:7,500 dilution; Sigma) was used as a control for equal loading of the cardiac homogenates.

RESULTS

MLP binds to CFL2 in cardiac and skeletal muscle homogenates. The CFL2 and MLP proteins are both expressed in human cardiac and skeletal (quadriceps) muscle (Fig. 1A). A CFL2 construct containing the full-length protein (aa 1 to 166) was expressed as a GST fusion protein (~45.5 kDa) in *E. coli* (Fig. 1B). Equivalent amounts of the GST-CFL2 fusion protein or control GST (~25 kDa) protein bound in glutathione matrices were incubated with human cardiac or human skeletal muscle homogenates. The matrix-bound GST fusion proteins were examined by Western blotting for their ability to bind MLP in these homogenates. Only the GST-CFL2 "pulled down" the endogenous MLP, whereas GST alone was unable to interact with MLP (Fig. 1C). It therefore appears that CFL2 and MLP may interact in vivo in both cardiac and skeletal muscles.

The interaction of MLP and CFL2 is direct. In order to assess whether the interaction between MLP and CFL2 is direct, we performed a series of in vitro binding assays. Bacterially expressed MBP-MLP (~64.5 kDa) bound to amylose resin matrices (Fig. 1D) was incubated with equivalent amounts of affinity-purified GST-CFL2 or control GST affinity-purified fusion proteins. Western blot analysis with a GST antibody demonstrated that MBP-MLP bound specifically to GST-CFL2 while no interaction was observed with the control GST protein (Fig. 1E, left panel). In a parallel set of experiments, GST-CFL2 bound to glutathione matrices was incubated with equivalent amounts of MBP-MLP or MBP affinity-purified proteins. Probing with an MBP antibody confirmed the direct and specific interaction of CFL2 and MLP (Fig. 1E, right panel). These findings therefore suggest that the interaction between MLP and CFL2 occurs independently of other proteins.

Identification of the interacting domains between MLP and CFL2. To identify the protein domains involved in the interaction between CFL2 and MLP, we performed blot overlay assays using three deletion constructs for each protein, fused to GST and MBP, respectively. In particular, we generated constructs containing CFL2 amino-terminal GST-CFL2-A (aa 1 to 55); central GST-CFL2-B (aa 55 to 108); and the carboxy-terminal domain GST-CFL2-C (aa 105 to 166) (Fig. 1F, left panel). In the case of MLP, we generated amino-terminal LIM1 MBP-MLP-LIM1 (aa 9 to 94); intermediate inter-LIM MBP-MLP-inter-LIM (aa 64 to 117); and the carboxy-terminal LIM2 domain MBP-MLP-LIM2 (aa 105 to 188) (Fig. 1F, right panel). By blot overlay assays, we determined that both the amino-terminal and central domains of CFL2 interact specifically with the inter-LIM domain of MLP (Fig. 1G). This is the first report of an MLP protein-protein interaction involving its inter-LIM domain.

MLP and CFL2 colocalize in vivo at the sarcomeric Z-line of human striated muscles. To determine the subcellular site of MLP-CFL2 interaction in striated muscles, we studied their localization in longitudinal sections of human quadriceps muscles using antibodies against MLP, CFL2, α-actinin, a marker for the Z-line, and phalloidin, a marker for thin filaments. Consistent with previous reports, MLP showed extensive costaining with α-actinin at the level of the sarcomeric Z-lines, supporting the notion that at least one of its roles in myocytes involves the myofibrillar structure (Fig. 2D) (9). CFL2 staining showed a similar striated pattern and was found to colocalize with α-actinin (Fig. 2B). Costaining of CFL2 and phalloidin confirmed their colocalization at the Z-disk but not across the full length of the thin filaments (Fig. 2C). Finally, costaining with anti-MLP and anti-CFL2 revealed that the two proteins colocalize in vivo at the Z-line of the sarcomeres (Fig. 2A).

The MLP-CFL2 interaction is pH sensitive. The pH-dependent interaction of cofilins with actin is an important property of the members of the ADF/cofilin family (38, 39). To deter-

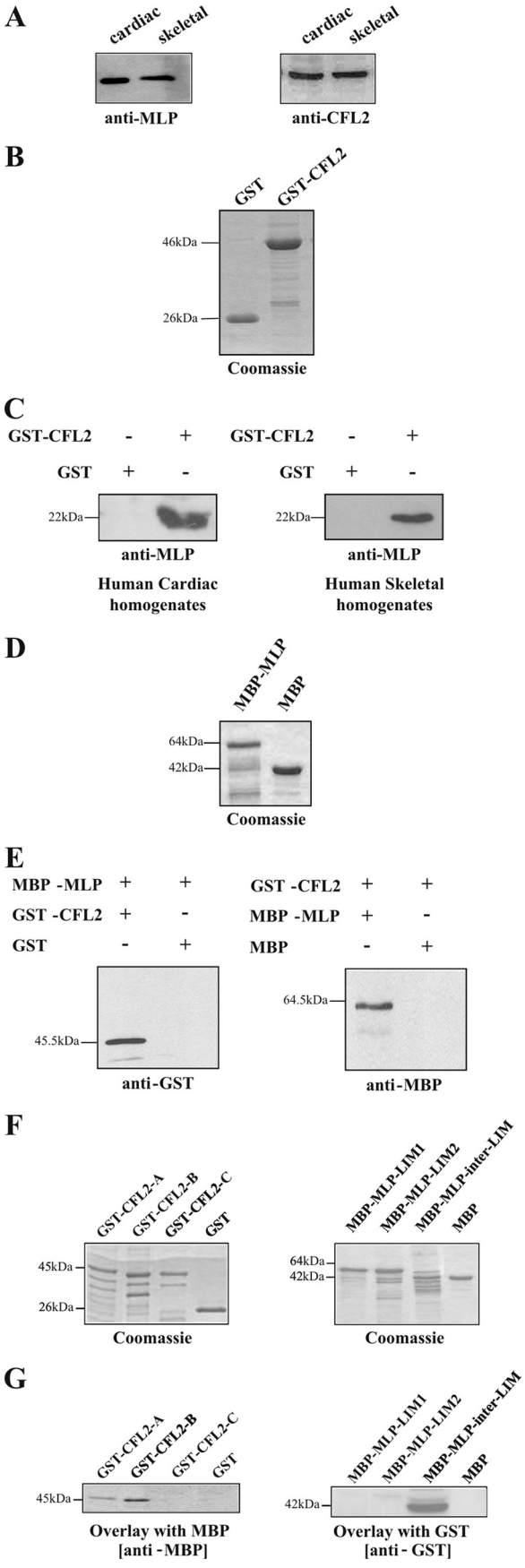

mine whether the interaction of MLP with CFL2 is affected by pH, we performed in vitro binding assays in which equal amounts of MBP-MLP or MBP bound on amylose resin were incubated with affinity-purified GST-CFL2 at different pH values. To reflect relative physiological and pathological pH conditions, like acidosis and alkalosis (67), we tested MLP/CFL2 complex formation at pH 6.8, pH 7.4, pH 8.0, and pH 8.5. Interestingly, the interaction between MLP and CFL2 was found to be pH sensitive, with maximal complex formation at pH 6.8 and minimal at pH 8.5 (Fig. 3A). Furthermore, the levels of MLP/CFL2 interaction were evaluated by quantitative immunoblotting. The graphical representation of the levels of MLP/CFL2 interaction against pH was well fitted to a sigmoid kinetic curve with a pK_a of 7.4 (Fig. 3B), as calculated with the Microcal Origin software program. Although pH dependent, the interaction between MLP and CFL2 was not completely abolished even at a high pH value, since 22% binding was detected at pH 8.5 compared to that at pH 6.8. The 50% of MLP/CFL2 interaction was found at pH 7.6, while at pH 7.3 and pH 7.4, which reflect the physiological intracellular pH in muscle (67), the binding strengths were estimated to be 78% and 69%, respectively. Therefore, MLP could bind to CFL2 under either acidic or alkaline conditions, although the interaction is stronger at acidic conditions (Fig. 3C).

MLP-CFL2 interaction is stronger when CFL2 is phosphorylated. Cofilin undergoes phosphorylation and dephosphorylation at Ser3, in response to various stimuli, affecting its binding properties for other proteins (2, 34, 62). To investigate whether the phosphorylation of CFL2 also influences its interaction with MLP, we phosphorylated the GST-CFL2 fusion protein using the native kinases in mouse heart homogenates. The phosphorylation was confirmed by Western blotting using a specific antibody against phosphorylated CFL2-Ser3 (Fig. 3D).

FIG. 1. CFL2 binds native MLP in cardiac and skeletal muscle homogenates, as demonstrated by "pull-down" and in vitro binding assays. (A) Western blot analysis showed that MLP (left) and CFL2 (right) are expressed in human cardiac and skeletal (quadriceps) muscle homogenates. (B) Recombinant GST-$CFL2_{aa1–166}$ (~46 kDa) and GST (~25 kDa) were separated by SDS-PAGE and visualized by staining with Coomassie brilliant blue. (C) For "pull-down" assays, human cardiac (left) or skeletal (right) muscle homogenates were incubated with equal amounts of GST-$CFL2_{aa1–166}$ and GST protein bound to glutathione matrices. Western blot analysis was performed with an anti-MLP antibody. (D) Recombinant MBP-$MLP_{aa1–195}$ and MBP (~42 kDa) were subjected to SDS-PAGE and stained with Coomassie brilliant blue. (E) Left panel: for in vitro binding assays, equal amounts of GST-CFL2 and GST were incubated with MBP-MLP bound to amylose resin beads. Binding of GST-CFL2 protein to MBP-MLP was determined by Western blot analysis with the anti-GST antibody. Right panel: equal amounts of MBP and MBP-MLP were incubated with GST-CFL2 attached to glutathione matrices. Western blotting with the anti-MBP antibody revealed that the MBP-MLP recombinant protein interacts with GST-CFL2. (F) Coomassie staining of the GST-generated constructs of CFL2 (left) or MBP-generated constructs of MLP (right). (G) Blot overlay assays were performed for the determination of the minimal domains of MLP and CFL2 required for their interaction. Left: blot overlay assays of CFL2 constructs attached to glutathione matrices after incubation with full-length MBP-MLP. Western blot analysis was performed with anti-MBP antibody. Right: blot overlay assays of MLP constructs attached to amylose resin matrices after incubation with full-length GST-CFL2, using the anti-GST antibody.

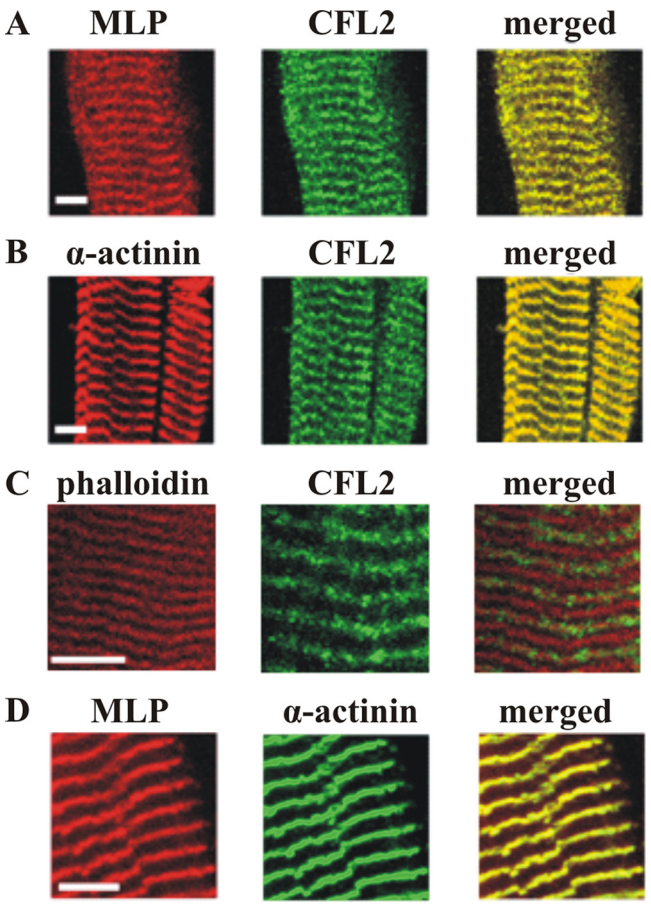

FIG. 2. In vivo localization of MLP and CFL2 at the Z-line of human skeletal muscle sections. (A) Coimmunolabeling of MLP and CFL2 with the specific antibodies shows that they interact in vivo at the Z-line of the sarcomere. (B) Immunostaining of α-actinin with CFL2 shows that the two proteins colocalize at the Z-line. (C) Costaining of CFL2 with rhodamine-phalloidin shows that CFL2 is not localized across the full length of the thin filaments. (D) MLP is localized at the Z-line, as shown with the colabeling with the marker of Z-line, α-actinin. Scale bar, 5 μm.

MBP-MLP was allowed to interact with equal amounts of phosphorylated and unphosphorylated GST-CFL2 in blot overlay assays. The results of three independent sets of experiments determined a significant increase of approximately 40% in the binding affinity of phosphorylated CFL2 for MLP compared to that of unphosphorylated CFL2 (Fig. 3E). Therefore, MLP appears to bind to both phosphorylated and unphosphorylated CFL2, although the interaction with the former is significantly stronger (Fig. 3F).

MLP-CFL2 interaction is independent of changes in Ca^{2+} concentration. Calcium is a versatile intracellular signal mediator that regulates many different cellular processes. In striated muscles, changes in the cytosolic Ca^{2+} concentration are key to the main muscle function of contraction/relaxation (52). Meanwhile, Ca^{2+} can mediate cofilin dephosphorylation, as described for numerous cell types, and is thought to contribute to various cell responses (15, 23, 88). We explored if variations in Ca^{2+} levels influence the binding of CFL2 to MLP. For this purpose, a series of Ca^{2+} titration blot overlay assays were performed using low (10^{-8} M), intermediate (10^{-7} and 10^{-6} M), and high (10^{-5} M) Ca^{2+} concentrations, which were selected to reflect physiologically relevant cytosolic Ca^{2+} concentrations in muscle (52). Quantification analysis of three replicate experiments revealed that the in vitro interaction of CFL2 with MLP is independent of Ca^{2+} concentrations (Fig. 3G and H). Thus, MLP/CFL2 complex formation seems to be independent of cytosolic Ca^{2+} changes, such as those occurring during muscle contraction/relaxation.

MLP regulates CFL2 depolymerization of F-actin. Proteins of the ADF/cofilin family are potent regulators of actin dynamics, and CFL2 is a key player in actin depolymerization (17). To test if the interaction between MLP and CFL2 interferes with this mechanism, we performed an in vitro pyrene–F-actin depolymerization assay, using recombinant MBP-MLP and GST-CFL2 proteins at pH 8.0 (starting pH recommended by the kit manufacturer). In these assays, pyrene G-actin is initially polymerized into fluorescent filamentous F-actin, an unstable structure that is subsequently allowed to depolymerize. The depolymerization process is monitored in real time and recorded as a decrease in the pyrene fluorescence signal. When GST-CFL2 was added to the reaction mixture, the depolymerization rate was accelerated as expected ($P < 0.001$, t test, two-tailed; $n = 3$). Addition of equivalent amounts of recombinant MBP-MLP significantly accelerated F-actin depolymerization compared to the activity of CFL2 alone ($P = 0.002$, t test, two-tailed; $n = 3$) (Fig. 4A). Importantly, the stoichiometry of MLP and CFL2 was found to have a major impact on the rate of F-actin depolymerization. Calculation of the slope of F-actin depolymerization relative to the MLP/CFL2 molecular ratio demonstrates a maximum effect at a 2:1 ratio (Fig. 4B). Interestingly, as we determined above, MLP can bind to two distinct domains of CFL2, suggesting a possibly simultaneous interaction of two MLP molecules with one CFL2. A higher molecular ratio of 3:1 MLP/CFL2 showed effects on F-actin depolymerization similar to those of 1:1 MLP/CFL2, while surprisingly, a ratio of 4:1 led to significant suppression of CFL2 activity on F-actin ($P = 0.003$, t test, two-tailed; $n = 3$). These findings suggest that the MLP/CFL2 molecular ratio is an important determinant of the rate of F-actin depolymerization, with important implications in muscle cell physiology and pathophysiology.

The minimal interacting domain of MLP does not suffice for mediating CFL2 F-actin depolymerization activity. To investigate whether the minimal interacting domain of MLP alone can affect CFL2 depolymerization activity, we performed in vitro depolymerization assays using the recombinant proteins MBP-MLP, MBP-inter-LIM, and GST-CFL2 under optimal conditions, i.e., at pH 8.0 and a MLP/CFL2 molecular ratio of 2:1. In contrast to the full-length MLP, we found that the inter-LIM domain per se does not affect the CFL2 F-actin depolymerization curve (Fig. 5A). This was further supported by evidence of a significant difference in the slope of CFL2-driven F-actin depolymerization in the presence of the MLP-inter-LIM domain or full-length MLP ($P = 0.003$, t test, two-tailed; $n = 3$) (Fig. 5B). These date combined imply the need of additional MLP domains for regulation of the CFL2 activity.

MLP rescues CFL2 depolymerization of F-actin at low pH. pH-dependent F-actin depolymerization is an important property of the members of the ADF/cofilin family and is maximal at pH 8.0 and almost abolished at pH 6.5 (38, 39). To evaluate

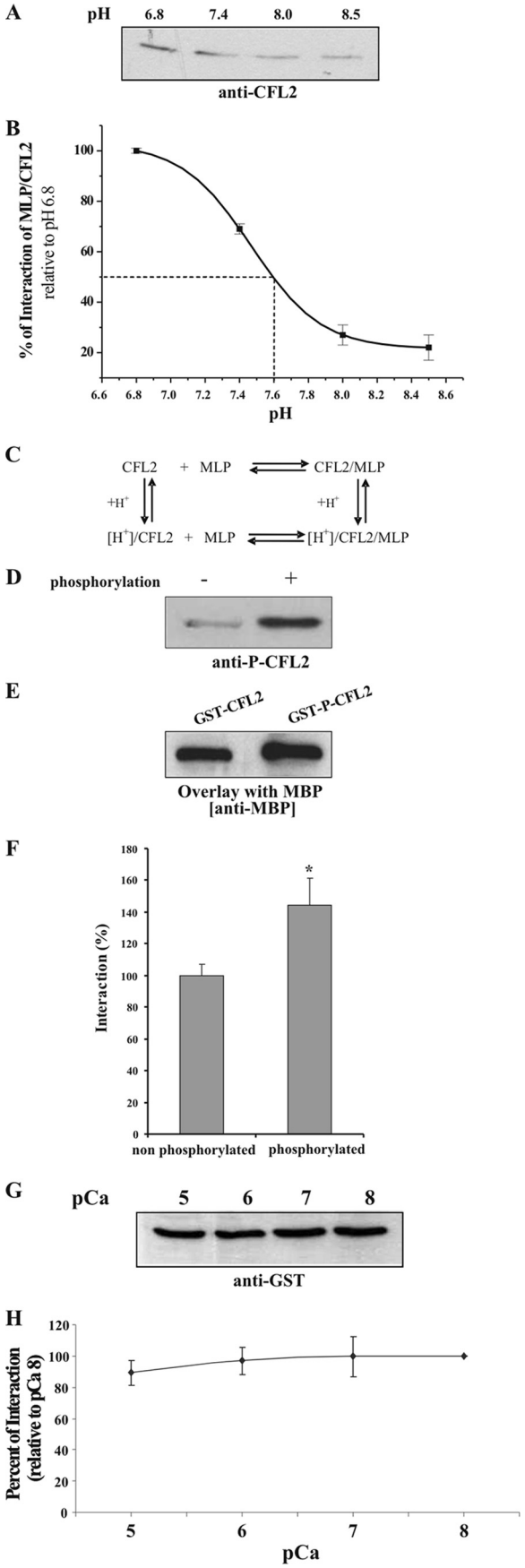

the effect of MLP on CFL2-dependent F-actin depolymerization in an acidic environment, we used the in vitro pyrene–F-actin depolymerization assay, at pH 6.8, with a 2:1 ratio of recombinant MBP-MLP/GST-CFL2. Similar to our observations with an alkaline environment (pH 8.0), the addition of MLP significantly increased the effect of CFL2 on F-actin depolymerization at pH 6.8 ($P = 0.003$, t test, two-tailed; $n = 3$) (Fig. 5C). Importantly, the presence of MLP at pH 6.8 appeared to restore the CFL2 F-actin depolymerization activity to the same levels as that for CFL2 alone at pH 8.0 (Fig. 5C and D, left panel). Finally, comparison of the effects of MLP on CFL2-dependent F-actin depolymerization at different pH levels did not show a statistically significant difference, indicating that this MLP effect is independent of the pH ($P = 0.102$, t test, two-tailed; $n = 3$) (Fig. 5D, right panel).

MLP has a limited effect on F-actin depolymerization upon CFL2 phosphorylation. The activity of cofilin is negatively regulated by phosphorylation (2, 62). To evaluate the effect of CFL2 phosphorylation on MLP/CFL2 F-actin depolymerization, we performed in vitro depolymerization assays using phosphorylated CFL2 at optimal conditions, pH 8.0 and an MLP/CFL2 molecular ratio of 2:1 (Fig. 5E). As opposed to unphosphorylated CFL2, phosphorylated CFL2 alone had no effect on F-actin depolymerization ($P = 0.002$, t test, two-tailed; $n = 3$). The addition of MLP showed a limited, nonsignificant increase in F-actin depolymerization, but it did not fully rescue the CFL2 activity (Fig. 5E).

Evaluation of CFL2-MLP interaction in a mouse model of cardiomyopathy. The interaction of CFL2 and MLP could be implicated in muscle pathologies. To investigate this hypothesis, we used the $Des^{-/-}$ mouse model, which develops dilated

FIG. 3. In vitro, the interaction of MLP with CFL2 is pH dependent and is stronger when CFL2 is phosphorylated but is not affected by alterations in calcium concentrations. (A) In vitro binding assays between full-length MBP-MLP, attached to amylose resin beads, and GST-CFL2 at different pH levels (from 6.8 to 8.5). The interaction was evaluated by Western blot analysis with the anti-CFL2 antibody. (B) A graphical representation of the levels of MLP/CFL2 interaction against pH fits well to a sigmoid kinetic curve, with a pK_α of 7.4. (C) Schematic model of the MLP/CFL2 interaction according to the protonation/deprotonation status of CFL2. (D) In vitro phosphorylation assays were performed using mouse cardiac homogenates. The native kinases present in the homogenate phosphorylate the GST-generated full-length CFL2, as shown by Western blot analysis with the specific anti-phospho-CFL2 antibody before (left) and after (right) the assay. (E) Equivalent amounts of phosphorylated and unphosphorylated GST-CFL2 were subjected to SDS-PAGE, transferred to nitrocellulose membranes, and incubated with recombinant MBP-MLP. Bound MBP-MLP was detected by Western blotting with anti-MBP antibody. (F) Graphical representation of the MLP/CFL2 interaction before and after phosphorylation. The results of three independent sets of experiments pointed to a significant increase of approximately 40% in the binding strength of phosphorylated CFL2 with MLP, compared to results for unphosphorylated CFL2. (G) In vitro assays were performed to explore if the interaction of MLP and CFL2 was affected by alterations in calcium concentrations. For this purpose, equal amounts of GST-CFL2 and MBP-MLP bound to amylose resin beads were incubated at various pCa concentrations (5 to 8, representing concentrations of 10^{-5} M to 10^{-8} M). Western blot analysis with the anti-GST antibody shows that the interaction of the complex is not affected by the calcium concentration. (H) Graphical representation of the interaction of the two proteins at various concentrations of calcium.

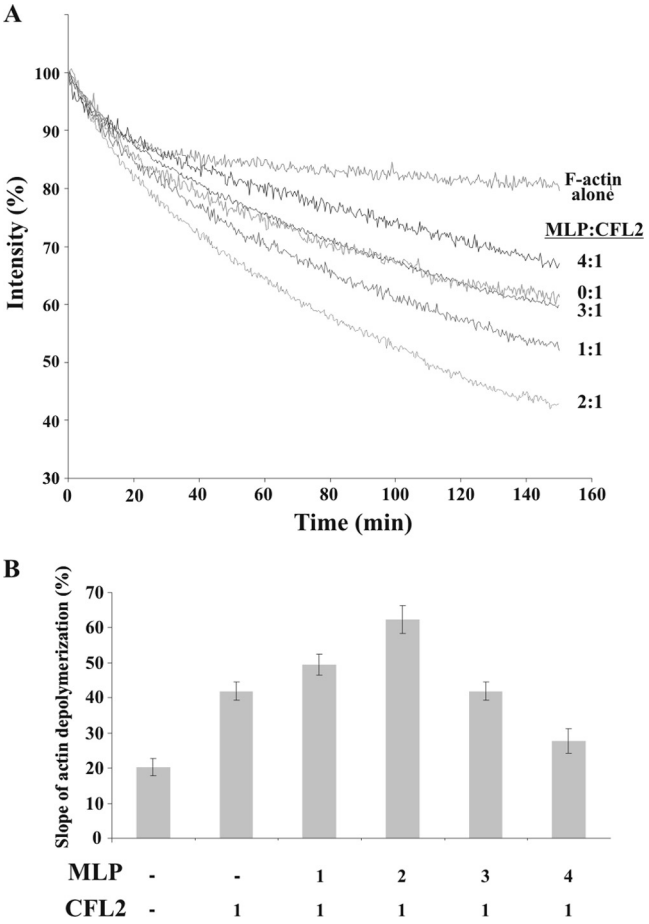

FIG. 4. MLP regulates CFL2 F-actin depolymerization. (A) In vitro depolymerization assays at pH 8.0 show how the presence of various concentrations of MBP-MLP (from 0.5 μM to 2 μM) affects GST-CFL2 F-actin depolymerization over time. (B) Calculation of the slope of F-actin depolymerization relative to the MLP/CFL2 molecular ratio. A maximal effect of F-actin depolymerization was seen at a 2:1 ratio ($P = 0.014$, t test, two-tailed; $n = 3$), while a ratio of 4:1 led to significant suppression of CFL2 activity on F-actin ($P = 0.003$, t test, two-tailed; $n = 3$) compared to results with the 1:1 ratio.

cardiomyopathy (28, 59). Specifically, cardiac protein extracts from wild-type and $Des^{-/-}$ mice were coimmunoprecipitated with protein A-Sepharose beads bound to anti-CFL2 antibody and subsequently analyzed by Western blotting (Fig. 6A) using the MLP antibody. Our findings demonstrate that MLP interacts with CFL2 in both wild-type and $Des^{-/-}$ hearts. However, the observed signal was markedly increased in the $Des^{-/-}$ cardiac homogenates. We further evaluated the protein levels of MLP and CFL2 through Western blot analysis in the cardiac homogenates and determined a considerable increase in MLP, while CFL2 remained unaltered between the $Des^{-/-}$ and wild-type cardiac homogenates (Fig. 6B).

DISCUSSION

We identified herein MLP as a novel binding partner of CFL2 in human cardiac and skeletal muscles. This interaction was evidenced by GST pull-down experiments with cardiac and skeletal muscle homogenates, in vitro blot overlay assays, and subcellular colocalization in human skeletal muscles. The interaction is direct and specific, and it implicates, for the first time, the inter-LIM domain of MLP as well as two domains of CFL2, suggesting that these two proteins may be part of a larger protein complex. Furthermore, this interaction appears to be regulated by pH and phosphorylation. Importantly, it is directly involved in F-actin depolymerization, thus unveiling a new mechanism of actin dynamics regulation. The MLP/CFL2 complex is therefore anticipated to play a significant role in cardiac and skeletal muscle function and in disease pathogenesis.

In previous reports, MLP localization had not been clearly defined, and several different patterns of MLP subcellular distribution had been suggested, including the Z-line (46), the costameres (27), a diffuse localization in the cytosol (31), or a translocation to the nucleus (16). It has been proposed that the use of polyclonal rabbit antisera affects the MLP localization findings, since these antibodies have the risk of unspecific binding on top of cross-reaction with other members of the LIM family of proteins (29). Herein, we used the polyclonal chicken-generated anti-MLP, immunoglobulin Y antibodies to reduce the possibility of unspecific binding. Using appropriate markers, we have demonstrated a Z-line distribution of MLP and CFL2 and have determined their colocalization. CFL2 was previously found to colocalize with actin (63), suggesting an I-band distribution. Our findings have narrowed down CFL2 localization to the Z-line of human skeletal myocytes.

Importantly, the protein domains of MLP involved in the interaction with CFL2 were determined to include amino acids 94 to 105, which represent the inter-LIM domain. While several binding partners of MLP have been identified to date, the vast majority involve one of the two LIM domains of MLP. These include interaction between MLP molecules (89), interaction with α-actinin (30), MyoD (47), histone deacetylases (36), F-actin (7), βI-spectrin (27), zyxin (51) and integrin-linked kinase (69). To the best to our knowledge, this is the first report implicating the inter-LIM domain in an MLP protein-protein interaction. This finding leads to the hypothesis of a scaffold multimeric organization of the MLP/CFL2 complex with other MLP-LIM-interacting proteins, similar to the model of simultaneous MLP interaction with βI-spectrin and α-actinin (27).

The CFL2 region involved in the interaction with MLP includes the N-terminal aa 1 to 105. Importantly, two separate fractions, 1 to 55 and 55 to 105, of this region can bind independently to MLP (Fig. 7). The first domain contains the CFL2 phosphorylation site (Ser-3) (2, 61), the first of the two G/F-actin interacting domains (aa 3 to 12) (34), and the N-terminal first third of the actin depolymerization (ADF) domain (65). The second fraction contains the middle part of the ADF domain, including aa 93 to 97, which are involved in F-actin binding (34). Two additional actin binding sites have been reported on cofilin, the C-terminal G/F-actin interacting domain (aa 109 to 141) and the F-actin binding responsible elements (aa 149 to 157) (34), but based on our findings these domains are not directly implicated in the MLP/CFL2 interaction. The interaction of two different CFL2 fractions with the inter-LIM domain of MLP suggests the presence of two independent surfaces on CFL2 for MLP, thus raising the possibility that two MLP molecules may interact with each CFL2.

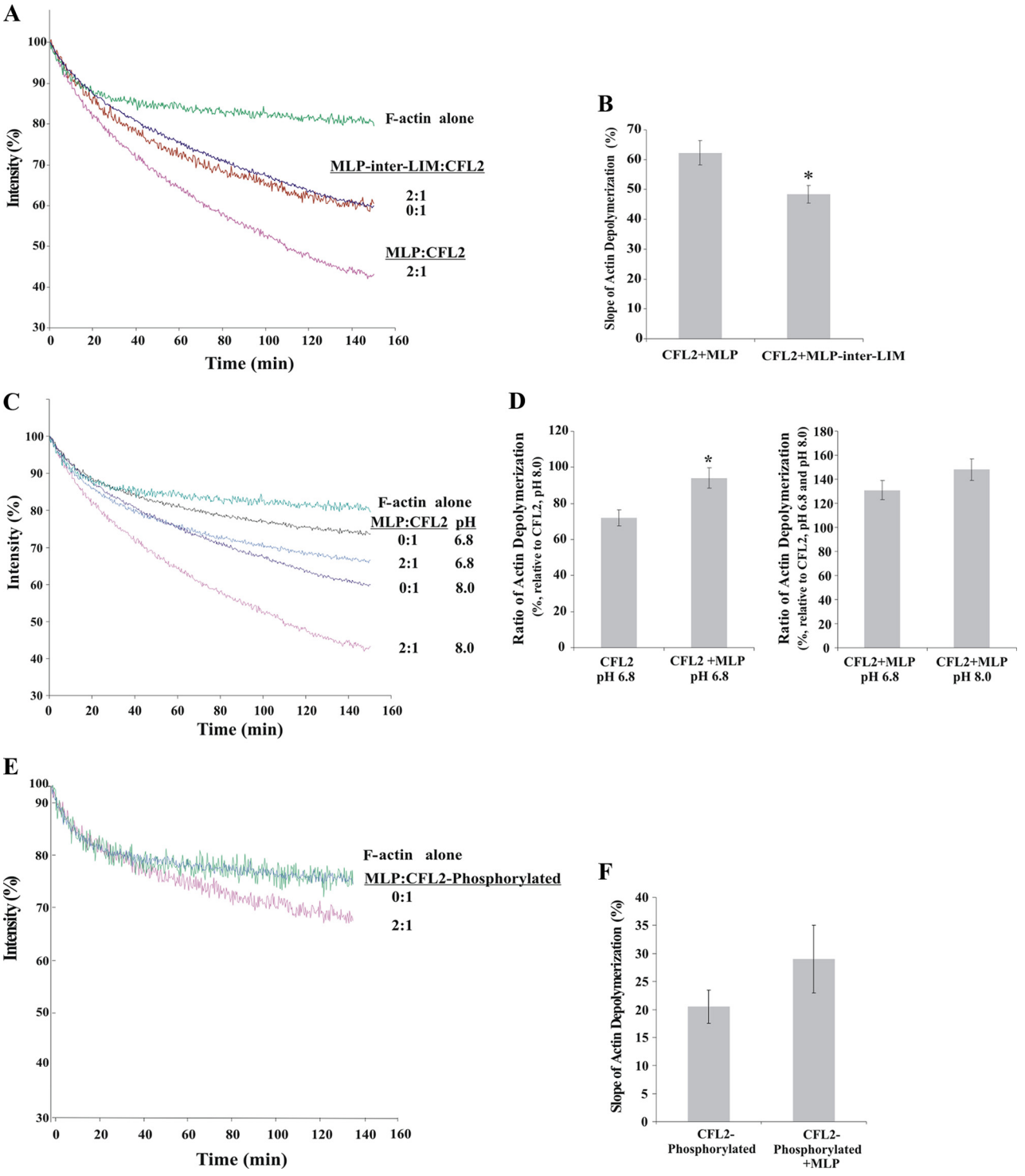

FIG. 5. Role of the MLP-inter-LIM domain, acidic pH, and phosphorylation in in vitro pyrene–F-actin depolymerization. (A) In vitro depolymerization assays at pH 8.0 in the presence of MBP-MLP or MLP-inter-LIM-MBP with CFL2-GST at a ratio of 2:1. (B) Graphical representation of the ratio of F-actin depolymerization in the presence of MLP and the MLP-inter-LIM domain alone. There was a significant difference between the effect of the full-length protein and that of the MLP-inter-LIM domain on F-actin depolymerization activity ($P = 0.003$, t test, two-tailed; $n = 3$). The MLP-inter-LIM domain is not sufficient for the regulation of CFL2-driven F-actin depolymerization. (C) Fluorescence experiments of F-actin depolymerization at pH 6.8 with a 2:1 ratio of recombinant MBP-MLP/GST-CFL2. The addition of MLP appeared to restore CFL2 F-actin depolymerization activity to the same levels as those for CFL2 alone at pH 8.0. (D) Left: graphical representation of the slope of F-actin depolymerization with or without the presence of MLP. The addition of MLP significantly increased the CFL2 effect on F-actin depolymerization ($P = 0.003$, t test, two-tailed; $n = 3$). Right: graphical representation of the slope of F-actin depolymerization by comparison of the MLP effect at different pH levels. We observed no statistically significant difference, indicating that this MLP effect is independent of the pH ($P = 0.102$, t test, two-tailed; $n = 3$). (E) In vitro F-actin depolymerization assays at pH 8.0 with a 2:1 ratio of recombinant MBP-MLP and phosphorylated GST-CFL2. (F) Graphical representation of the slope of F-actin depolymerization by comparison of phosphorylated GST-CFL2 in the presence or absence of MBP-MLP. No statistically significant changes were observed, suggesting that MLP has a limited effect on phosphorylated CFL2 F-actin depolymerization activity ($P = 0.002$, t test, two-tailed; $n = 3$).

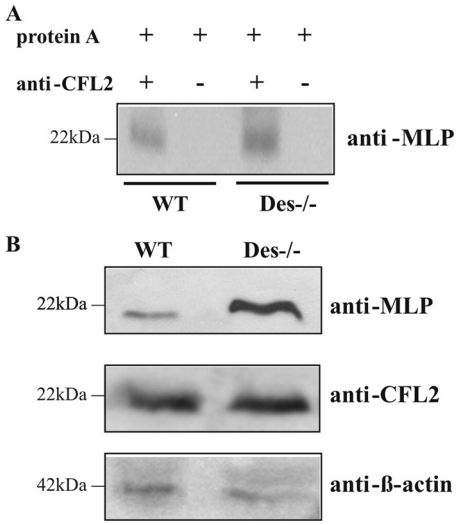

FIG. 6. Coimmunoprecipitation experiments with mouse cardiac homogenates. Coimmunoprecipitation was preformed with cardiac protein extracts from wild-type and $Des^{-/-}$ mice, using protein A-Sepharose beads bound to anti-CFL2 antibody. The resulting protein complex was then analyzed by Western blotting using antibodies against MLP. (A) MLP coprecipitated with CFL2 in wild-type and $Des^{-/-}$ cardiac homogenates, although the signal was increased in the latter. (B) Western blot experiments show increased levels of MLP but not of CFL2 in $Des^{-/-}$ samples. β-Actin was used as a loading control.

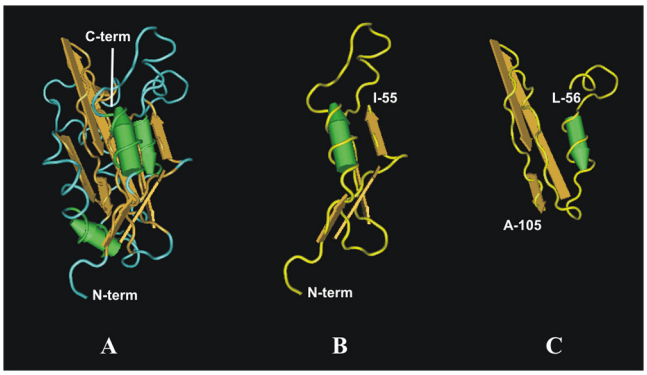

FIG. 7. Three-dimensional structure model of CFL2 using the Cn3D software program, adjusted from the nuclear magnetic resonance structure of human cofilin 1 (1Q8G). The MLP-interacting domains are depicted. (A) CFL2 aa 1 to 166 (blue). (B) CFL2 aa 1 to 55 (yellow). (C) CFL2 aa 56 to 105 (yellow). Alpha helixes are shown in green; beta sheets are shown in brown. C-term, C-terminal; N-term, N-terminal.

The activity of the ADF/cofilin proteins on actin is thought to be regulated by pH both in vitro (38, 39, 86, 87) and in living cells (14). Most of the ADF/cofilins exhibit stronger F-actin depolymerizing activity at alkaline pH values than in neutral to acidic environments (1, 18, 38, 39, 87). Specifically, they tend to bind more strongly with F-actin at pH 6.5 and with G-actin at pH 8.0 (42, 87). Our data indicate that the MLP/CFL2 interaction is stronger under relatively acidic conditions than in neutral and alkaline environments. The kinetic curve of MLP/CFL2 complex formation for different pH levels results in a sigmoid pattern that falls within the pK_a range of histidine (49). However, the only histidine residue in CFL2 is the conservative His-133, and it has been suggested by nuclear magnetic resonance studies of cofilin 1 that its protonation/deprotonation state results to three-dimensional conformation changes of the whole protein (68). Such a conformational change may therefore explain the pH sensitivity of the MLP/CFL2 complex. Overall, our results reveal that MLP could bind to either protonated or deprotonated CFL2, although this interaction is much stronger with the former (Fig. 3C). Therefore, changes of the physiological intracellular pH in the myocyte could affect MLP/CFL2 binding affinity, with implications for cardiac and skeletal muscle physiology (Fig. 8). Such changes in pH have been observed in skeletal muscle during acute high-intensity (66, 70) or chronic exercise (56) and in cardiac muscle during increased contraction rates of the heart.

Phosphorylation of ADF/cofilins affects their ability to interact with other proteins, such as actin (2, 62), or molecules, such as PIP_2 (34, 41). Four different kinases catalyze the phosphorylation of ADF/cofilins at Ser-3, namely, the LIM kinases, LIMK1 (6, 85) and LIMK2 (53, 74), and the testis-specific kinases TESK1 (77) and TESK2 (78). Dephosphorylation of ADF/cofilins is caused by several phosphatases, including type 1, type 2A (5), type 2B (58), type 2C (88), Slingshot phosphatase (64), and the novel cofilin phosphatase, chronophin (33). We showed that the phosphorylated CFL2 has an affinity for MLP that is increased by approximately 40% compared to that of the unphosphorylated form. Interestingly, since the CFL2 phosphorylation site at Ser-3 is present within the MLP/CFL2 interacting region, it is possible that the phosphorylation of CFL2 could enhance its interaction with MLP through electrostatic (62) or structural (34) changes. These findings unveil at least one aspect of the clinical significance of CFL2 phosphorylation changes under different physiological conditions, such as increased muscle stretch, where CFL2 phosphorylation increases (4) (Fig. 8).

Muscle contraction is regulated mainly by intracellular calcium ion (Ca^{2+}) changes, which affect excitation-contraction coupling (26) and the amplitude of the contractile force (12). Our analysis showed that the MLP/CFL2 interaction is independent of pCa alterations within the relevant physiological levels observed during muscle contraction/relaxation (52), suggesting that the MLP/CFL2 interaction could persist throughout the (cardio)myocyte contraction/relaxation cycle.

The main molecular function of ADF/cofilin family proteins, including CFL2, is the regulation of actin dynamics (6). Meanwhile, MLP can bind actin and has been suggested to participate in the regulation of actin cytoskeleton architecture (7), while other members of this family, namely, CRP1 and CRP2, have been linked with actin bundling (35, 79). The precise mechanisms of how MLP might be implicated in these processes have not been determined. We hypothesized that MLP, through its interaction with CFL2, might affect actin dynamics. For this reason, we examined F-actin depolymerization in the presence of both CFL2 and MLP. We found that the addition of an equal amount of MLP to CFL2 enhances the depolymerization of F-actin compared to that with CFL2 alone, indicating that the MLP/CFL2 complex can directly affect the F-actin cytoskeleton dynamics. The maximum effect of MLP on CFL2 F-actin depolymerization activity was observed at a molecular

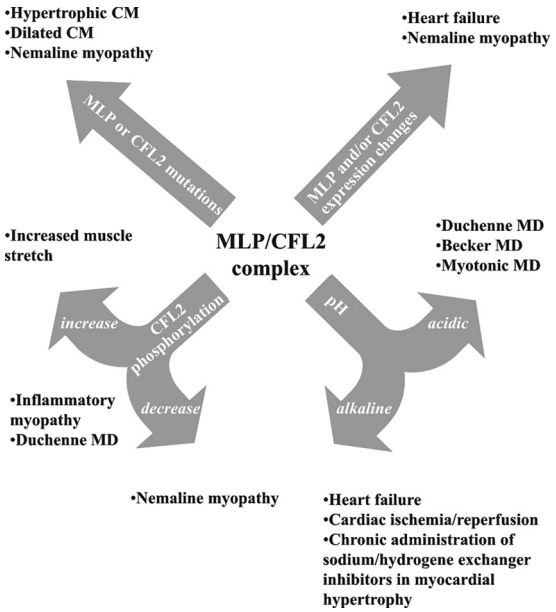

FIG. 8. Hypothetical model of the different mechanisms through which the MLP/CFL2 complex could contribute to the pathogenesis of cardiac and skeletal muscle diseases. Characteristic examples of such diseases for which mutations, expression changes, CFL2 phosphorylation, or intracellular pH level variations have been described are presented. MD, muscular dystrophy; CM, cardiomyopathy.

ratio of MLP/CFL2 equal to 2:1. This finding clarifies the importance of having two MLP binding sites on CFL2.

Higher ratios of MLP to CFL2 appear to have a decreasing F-actin depolymerization activity, with ratios of 3:1 returning the activity to baseline levels (the same as that with CFL2 alone) and ratios of 4:1 leading to suppressed depolymerization. The suppressive effects of MLP saturation on CFL2 F-actin depolymerization could be explained by MLP multimerization (16). Interestingly, MLP/MLP dimmers have been suggested to interact with F-actin and to stabilize its formation (7). Therefore, the development of a scaffold multimer at the Z-disk of the sarcomere between MLP and CFL2 may promote either depolymerization or stabilization of F-actin according to the complex stoichiometry.

The minimal interacting domain of MLP for CFL2 (MLP-inter-LIM) alone has no effect on CFL2-driven F-actin depolymerization in vitro under optimal conditions. The need for full-length MLP to regulate CFL2 activity suggests the involvement of multiple MLP domains in the regulation of CFL2 F-actin depolymerization. Furthermore, we found that phosphorylation of CFL2 abolishes its activity for F-actin depolymerization in vitro. In contrast to results with unphosphorylated CFL2, the presence of MLP has only a limited effect on phosphorylated CFL2 F-actin depolymerization activity. Interestingly, the rate of F-actin depolymerization in the presence of MLP and phosphorylated CFL2 at a 2:1 ratio was highly similar to that of MLP and unphosphorylated CFL2 at a 4:1 ratio. This observation is consistent with the increased binding of MLP to phosphorylated CFL2 and suggests that although the presence of MLP overall promotes CFL2 F-actin depolymerization, increased binding of MLP and CFL2 reverses this effect. Importantly, in addition to unveiling a novel molecular aspect of (cardio)myocyte physiology, this interaction of MLP with CFL2, its regulation by CFL2 phosphorylation and pH levels, and its direct implication in actin dynamics shed light on the elusive mechanisms of cardiac and skeletal muscle disease pathogenesis.

Specifically, the histological characteristics of NM are indicative of perturbations in actin dynamics which, based on our findings, could be the outcome of MLP/CFL2 complex aberrations. In support of this, the recently identified, first NM causative mutation in CFL2 involved an amino acid substitution (Ala35Thr) shown to significantly change the CFL2 conformation, leading to reduced stability or degradation of the CFL2 protein (3). Furthermore, MLP overexpression, a consistent finding in NM skeletal muscles (72), would also be expected to disturb intracellular MLP/CFL2 ratios. Similarly, MLP mutations have been associated with DCM and HCM, which is occasionally accompanied by skeletal myopathy (9, 31, 32, 46). In these cases the myofibers display severe cytoarchitectural perturbations and sarcomeric disarray, which could be explained by the structural or stoichiometric aberrations in MLP/CFL2 complex formation. Imbalances in this delicately regulated system through function-altering mutations or expression changes could have deleterious consequences for the actin cytoskeleton and myocyte function, ultimately leading to the (cardio)myopathic phenotype (Fig. 8). Future studies will explore the validity of this hypothesis with suitable disease models.

The clinical importance of the MLP/CFL2 interaction in striated muscle physiology and pathophysiology is further emphasized by the enhancement of CFL2 F-actin depolymerization activity at acidic pH upon MLP addition. While it is well documented that CFL2 exhibits diminished actin depolymerization activity at a pH of <7.0 (1, 18, 38, 39, 87), our data showed that the presence of specific MLP concentrations restores the CFL2 actin depolymerization activity to its pH 8.0 levels (Fig. 5). This can be explained by the stronger interaction of MLP with CFL2 under acidic conditions (Fig. 3). Reduced intracellular pH levels have been found in a variety of different diseases, such as heart failure (44), cardiac ischemia/reperfusion (21), chronic administration of sodium/hydrogen exchanger selective inhibitors in myocardial hypertrophy (11, 20, 43), and chronic acidosis. Meanwhile, abnormally increased pH levels have been detected in certain muscular dystrophies (e.g., Duchenne, Becker, and myotonic) (45, 50, 75). These disease-related pH changes would be anticipated to affect MLP/CFL2 interaction and actin depolymerization, with direct implications for myocyte cytoarchitecture and function (Fig. 8).

Finally, the observed effect of CFL2 phosphorylation on the MLP/CFL2 interaction is likely to represent yet another role for this complex in disease pathogenesis, since it can vary considerably under different conditions. Specifically, phosphorylated CFL2 is undetectable in the skeletal muscles of NM patients (3), and LIMK2 is significantly changed in Duchenne muscular dystrophy patients (37). CFL2 phosphorylation is also significantly reduced in smooth muscles following exposure to inflammatory mediators, such as platelet-derived growth factor, interleukin 1β, ET1, and tumor necrosis factor alpha (22). Of note, inflammation is a hallmark of numerous

types of myopathy (e.g., inflammatory myopathy) and dystrophy (e.g., Duchenne).

To evaluate the potential involvement of the MLP/CFL2 complex in muscle pathology, we used the $Des^{-/-}$ mouse model, which presents with dilated cardiomyopathy and ultimately heart failure (28). Our findings demonstrate that CFL2 protein expression levels remain unchanged while MLP is markedly increased, similar to other myopathy models (71, 82). Coimmunoprecipitations using the CFL2 antibody showed an increase in the levels of the MLP/CFL2 complex, indicating that an excess of MLP was bound to CFL2. These data suggest a change in the MLP/CFL2 stoichiometry, potentially altering F-actin dynamics through modification of CFL2 activity, and implicate this novel protein complex in the $Des^{-/-}$ mouse model of cardiomyopathy. Future studies will need to explore exactly how the MLP/CFL2 complex might be affected in other cardiomyopathies and skeletal myopathies.

In conclusion, we showed that CFL2 is a novel binding partner of MLP. This interaction has direct implications in F-actin depolymerization, and it could serve as one of the underlying mechanisms maintaining actin dynamics. The stoichiometry of this complex appears to be critical for its activity, which is optimal at MLP/CFL2 ratios equal to 2:1. The discovery of the MLP/CFL2 complex and its role in actin depolymerization contributes to a better understanding not only of myocyte molecular physiology but more importantly of the pathogenic mechanisms involved in a range of cardiac and skeletal muscle diseases. Perturbations in MLP/CFL2 complex formation or stoichiometry by mutations or altered expression, such as those we observed in the $Des^{-/-}$ mouse model for cardiomyopathy, are expected to directly affect the actin cytoskeleton and myocyte function. Further work will explore the possible therapeutic significance of the MLP/CFL2 interaction in striated muscle diseases.

ACKNOWLEDGMENTS

We thank Yassemi Capetanaki, Stelios Psarras, and Ioanna Kostavasili for providing us with the $Des^{-/-}$ mouse model.

This study was supported by research funds from the Biomedical Research Foundation of the Academy of Athens, the Hellenic Cardiological Society, the John F. Kostopoulos Foundation, NIH HL26057, HL64018, and HL77101, and the Leducq Foundation Trans-Atlantic alliance. E.V. and D.S. are supported by the European Union 6th Framework Program for Research and Technological Development, "Life sciences, genomics and biotechnology for health," VALAPODYN, contract no. LSHG-CT-2006-037277.

We have no conflict of interest to declare.

REFERENCES

1. **Abe, H., R. Nagaoka, and T. Obinata.** 1993. Cytoplasmic localization and nuclear transport of cofilin in cultured myotubes. Exp. Cell Res. **206:**1–10.
2. **Agnew, B. J., L. S. Minamide, and J. R. Bamburg.** 1995. Reactivation of phosphorylated actin depolymerizing factor and identification of the regulatory site. J. Biol. Chem. **270:**17582–17587.
3. **Agrawal, P. B., R. S. Greenleaf, K. K. Tomczak, V. L. Lehtokari, C. Wallgren-Pettersson, W. Wallefeld, N. G. Laing, B. T. Darras, S. K. Maciver, P. R. Dormitzer, and A. H. Beggs.** 2007. Nemaline myopathy with minicores caused by mutation of the CFL2 gene encoding the skeletal muscle actin-binding protein, cofilin-2. Am. J. Hum. Genet. **80:**162–167.
4. **Albinsson, S., I. Nordstrom, and P. Hellstrand.** 2004. Stretch of the vascular wall induces smooth muscle differentiation by promoting actin polymerization. J. Biol. Chem. **279:**34849–34855.
5. **Ambach, A., J. Saunus, M. Konstandin, S. Wesselborg, S. C. Meuer, and Y. Samstag.** 2000. The serine phosphatases PP1 and PP2A associate with and activate the actin-binding protein cofilin in human T lymphocytes. Eur. J. Immunol. **30:**3422–3431.
6. **Arber, S., F. A. Barbayannis, H. Hanser, C. Schneider, C. A. Stanyon, O. Bernard, and P. Caroni.** 1998. Regulation of actin dynamics through phosphorylation of cofilin by LIM-kinase. Nature **393:**805–809.
7. **Arber, S., and P. Caroni.** 1996. Specificity of single LIM motifs in targeting and LIM/LIM interactions in situ. Genes Dev. **10:**289–300.
8. **Arber, S., G. Halder, and P. Caroni.** 1994. Muscle LIM protein, a novel essential regulator of myogenesis, promotes myogenic differentiation. Cell **79:**221–231.
9. **Arber, S., J. J. Hunter, J. Ross, Jr., M. Hongo, G. Sansig, J. Borg, J. C. Perriard, K. R. Chien, and P. Caroni.** 1997. MLP-deficient mice exhibit a disruption of cardiac cytoarchitectural organization, dilated cardiomyopathy, and heart failure. Cell **88:**393–403.
10. **Arvanitis, D. A., E. Vafiadaki, G. C. Fan, B. A. Mitton, K. N. Gregory, F. Del Monte, A. Kontrogianni-Konstantopoulos, D. Sanoudou, and E. G. Kranias.** 2007. Histidine-rich Ca-binding protein interacts with sarcoplasmic reticulum Ca-ATPase. Am. J. Physiol. Heart Circ. Physiol. **293:**H1581–H1589.
11. **Baartscheer, A., M. Hardziyenka, C. A. Schumacher, C. N. Belterman, M. M. van Borren, A. O. Verkerk, R. Coronel, and J. W. Fiolet.** 2008. Chronic inhibition of the Na+/H+-exchanger causes regression of hypertrophy, heart failure, and ionic and electrophysiological remodelling. Br. J. Pharmacol. **154:**1266–1275.
12. **Bassani, R. A., J. W. Bassani, and D. M. Bers.** 1994. Relaxation in ferret ventricular myocytes: unusual interplay among calcium transport systems. J. Physiol. **476:**295–308.
13. **Beatham, J., K. Gehmlich, P. F. van der Ven, J. Sarparanta, D. Williams, P. Underhill, C. Geier, D. O. Furst, B. Udd, and G. Blanco.** 2006. Constitutive upregulations of titin-based signalling proteins in KY deficient muscles. Neuromuscul. Disord. **16:**437–445.
14. **Bernstein, B. W., W. B. Painter, H. Chen, L. S. Minamide, H. Abe, and J. R. Bamburg.** 2000. Intracellular pH modulation of ADF/cofilin proteins. Cell Motil. Cytoskeleton **47:**319–336.
15. **Birkenfeld, J., B. Kartmann, H. Betz, and D. Roth.** 2001. Cofilin activation during Ca(2+)-triggered secretion from adrenal chromaffin cells. Biochem. Biophys. Res. Commun. **286:**493–498.
16. **Boateng, S. Y., R. J. Belin, D. L. Geenen, K. B. Margulies, J. L. Martin, M. Hoshijima, P. P. de Tombe, and B. Russell.** 2007. Cardiac dysfunction and heart failure are associated with abnormalities in the subcellular distribution and amounts of oligomeric muscle LIM protein. Am. J. Physiol. Heart Circ. Physiol. **292:**H259–J269.
17. **Carlier, M. F., S. Wiesner, C. Le Clainche, and D. Pantaloni.** 2003. Actin-based motility as a self-organized system: mechanism and reconstitution in vitro. C. R. Biol. **326:**161–170.
18. **Chen, H., B. W. Bernstein, J. M. Sneider, J. A. Boyle, L. S. Minamide, and J. R. Bamburg.** 2004. In vitro activity differences between proteins of the ADF/cofilin family define two distinct subgroups. Biochemistry **43:**7127–7142.
19. **Chu, A., C. Sumbilla, G. Inesi, S. D. Jay, and K. P. Campbell.** 1990. Specific association of calmodulin-dependent protein kinase and related substrates with the junctional sarcoplasmic reticulum of skeletal muscle. Biochemistry **29:**5899–5905.
20. **Cingolani, H. E., and I. L. Ennis.** 2007. Sodium-hydrogen exchanger, cardiac overload, and myocardial hypertrophy. Circulation **115:**1090–1100.
21. **Crake, T., P. A. Crean, L. M. Shapiro, A. F. Rickards, and P. A. Poole-Wilson.** 1987. Coronary sinus pH during percutaneous transluminal coronary angioplasty: early development of acidosis during myocardial ischaemia in man. Br. Heart J. **58:**110–115.
22. **Dai, Y. P., S. Bongalon, H. Tian, S. D. Parks, V. N. Mutafova-Yambolieva, and I. A. Yamboliev.** 2006. Upregulation of profilin, cofilin-2 and LIMK2 in cultured pulmonary artery smooth muscle cells and in pulmonary arteries of monocrotaline-treated rats. Vascul. Pharmacol. **44:**275–282.
23. **Davidson, M. M., and R. J. Haslam.** 1994. Dephosphorylation of cofilin in stimulated platelets: roles for a GTP-binding protein and Ca2+. Biochem. J. **301:**41–47.
24. **Ecarnot-Laubriet, A., K. De Luca, D. Vandroux, M. Moisant, C. Bernard, M. Assem, L. Rochette, and J. R. Teyssier.** 2000. Downregulation and nuclear relocation of MLP during the progression of right ventricular hypertrophy induced by chronic pressure overload. J. Mol. Cell Cardiol. **32:**2385–2395.
25. **Ehler, E., R. Horowits, C. Zuppinger, R. L. Price, E. Perriard, M. Leu, P. Caroni, M. Sussman, H. M. Eppenberger, and J. C. Perriard.** 2001. Alterations at the intercalated disk associated with the absence of muscle LIM protein. J. Cell Biol. **153:**763–772.
26. **Fabiato, A., and F. Fabiato.** 1977. Calcium release from the sarcoplasmic reticulum. Circ. Res. **40:**119–129.
27. **Flick, M. J., and S. F. Konieczny.** 2000. The muscle regulatory and structural protein MLP is a cytoskeletal binding partner of betaI-spectrin. J. Cell Sci. **113:**1553–1564.
28. **Fountoulakis, M., E. Soumaka, K. Rapti, M. Mavroidis, G. Tsangaris, A. Maris, N. Weisleder, and Y. Capetanaki.** 2005. Alterations in the heart mitochondrial proteome in a desmin null heart failure model. J. Mol. Cell Cardiol. **38:**461–474.
29. **Gehmlich, K., C. Geier, H. Milting, D. Furst, and E. Ehler.** 2008. Back to

square one: what do we know about the functions of muscle LIM protein in the heart? J. Muscle Res. Cell Motil. **29:**155–158.
30. **Gehmlich, K., C. Geier, K. J. Osterziel, P. F. Van der Ven, and D. O. Furst.** 2004. Decreased interactions of mutant muscle LIM protein (MLP) with N-RAP and alpha-actinin and their implication for hypertrophic cardiomyopathy. Cell Tissue Res. **317:**129–136.
31. **Geier, C., K. Gehmlich, E. Ehler, S. Hassfeld, A. Perrot, K. Hayess, N. Cardim, K. Wenzel, B. Erdmann, F. Krackhardt, M. G. Posch, A. Bublak, H. Nagele, T. Scheffold, R. Dietz, K. R. Chien, S. Spuler, D. O. Furst, P. Nurnberg, and C. Ozcelik.** 2008. Beyond the sarcomere: *CSRP3* mutations cause hypertrophic cardiomyopathy. Hum. Mol. Genet. **17:**2753–2765.
32. **Geier, C., A. Perrot, C. Ozcelik, P. Binner, D. Counsell, K. Hoffmann, B. Pilz, Y. Martiniak, K. Gehmlich, P. F. van der Ven, D. O. Furst, A. Vornwald, E. von Hodenberg, P. Nurnberg, T. Scheffold, R. Dietz, and K. J. Osterziel.** 2003. Mutations in the human muscle LIM protein gene in families with hypertrophic cardiomyopathy. Circulation **107:**1390–1395.
33. **Gohla, A., J. Birkenfeld, and G. M. Bokoch.** 2005. Chronophin, a novel HAD-type serine protein phosphatase, regulates cofilin-dependent actin dynamics. Nat. Cell Biol. **7:**21–29.
34. **Gorbatyuk, V. Y., N. J. Nosworthy, S. A. Robson, N. P. Bains, M. W. Maciejewski, C. G. Dos Remedios, and G. F. King.** 2006. Mapping the phosphoinositide-binding site on chick cofilin explains how PIP2 regulates the cofilin-actin interaction. Mol. Cell **24:**511–522.
35. **Grubinger, M., and M. Gimona.** 2004. CRP2 is an autonomous actin-binding protein. FEBS Lett. **557:**88–92.
36. **Gupta, M. P., S. A. Samant, S. H. Smith, and S. G. Shroff.** 2008. HDAC4 and PCAF bind to cardiac sarcomeres and play a role in regulating myofilament contractile activity. J. Biol. Chem. **283:**10135–10146.
37. **Haslett, J. N., D. Sanoudou, A. T. Kho, R. R. Bennett, S. A. Greenberg, I. S. Kohane, A. H. Beggs, and L. M. Kunkel.** 2002. Gene expression comparison of biopsies from Duchenne muscular dystrophy (DMD) and normal skeletal muscle. Proc. Natl. Acad. Sci. USA **99:**15000–15005.
38. **Hawkins, M., B. Pope, S. K. Maciver, and A. G. Weeds.** 1993. Human actin depolymerizing factor mediates a pH-sensitive destruction of actin filaments. Biochemistry **32:**9985–9993.
39. **Hayden, S. M., P. S. Miller, A. Brauweiler, and J. R. Bamburg.** 1993. Analysis of the interactions of actin depolymerizing factor with G- and F-actin. Biochemistry **32:**9994–10004.
40. **Heineke, J., T. Kempf, T. Kraft, A. Hilfiker, H. Morawietz, R. J. Scheubel, P. Caroni, S. M. Lohmann, H. Drexler, and K. C. Wollert.** 2003. Downregulation of cytoskeletal muscle LIM protein by nitric oxide: impact on cardiac myocyte hypertrophy. Circulation **107:**1424–1432.
41. **Hosoda, A., N. Sato, R. Nagaoka, H. Abe, and T. Obinata.** 2007. Activity of cofilin can be regulated by a mechanism other than phosphorylation/dephosphorylation in muscle cells in culture. J. Muscle Res. Cell Motil. **28:**183–194.
42. **Iida, K., K. Moriyama, S. Matsumoto, H. Kawasaki, E. Nishida, and I. Yahara.** 1993. Isolation of a yeast essential gene, COF1, that encodes a homologue of mammalian cofilin, a low-M(r) actin-binding and depolymerizing protein. Gene. **124:**115–120.
43. **Karmazyn, M., A. Kilic, and S. Javadov.** 2008. The role of NHE-1 in myocardial hypertrophy and remodelling. J. Mol. Cell Cardiol. **44:**647–653.
44. **Katz, A. M., and H. H. Hecht.** 1969. Editorial: the early "pump" failure of the ischemic heart. Am. J. Med. **47:**497–502.
45. **Kemp, G. J., D. J. Taylor, J. F. Dunn, S. P. Frostick, and G. K. Radda.** 1993. Cellular energetics of dystrophic muscle. J. Neurol. Sci. **116:**201–206.
46. **Knoll, R., M. Hoshijima, H. M. Hoffman, V. Person, I. Lorenzen-Schmidt, M. L. Bang, T. Hayashi, N. Shiga, H. Yasukawa, W. Schaper, W. McKenna, M. Yokoyama, N. J. Schork, J. H. Omens, A. D. McCulloch, A. Kimura, C. C. Gregorio, W. Poller, J. Schaper, H. P. Schultheiss, and K. R. Chien.** 2002. The cardiac mechanical stretch sensor machinery involves a Z disc complex that is defective in a subset of human dilated cardiomyopathy. Cell **111:**943–955.
47. **Kong, Y., M. J. Flick, A. J. Kudla, and S. F. Konieczny.** 1997. Muscle LIM protein promotes myogenesis by enhancing the activity of MyoD. Mol. Cell. Biol. **17:**4750–4760.
48. **Kouloumenta, A., M. Mavroidis, and Y. Capetanaki.** 2007. Proper perinuclear localization of the TRIM-like protein myospryn requires its binding partner desmin. J. Biol. Chem. **282:**35211–35221.
49. **Li, H., A. D. Robertson, and J. H. Jensen.** 2005. Very fast empirical prediction and rationalization of protein pKa values. Proteins **61:**704–721.
50. **Lodi, R., G. J. Kemp, F. Muntoni, C. H. Thompson, C. Rae, J. Taylor, P. Styles, and D. J. Taylor.** 1999. Reduced cytosolic acidification during exercise suggests defective glycolytic activity in skeletal muscle of patients with Becker muscular dystrophy. An in vivo 31P magnetic resonance spectroscopy study. Brain **122:**121–130.
51. **Louis, H. A., J. D. Pino, K. L. Schmeichel, P. Pomies, and M. C. Beckerle.** 1997. Comparison of three members of the cysteine-rich protein family reveals functional conservation and divergent patterns of gene expression. J. Biol. Chem. **272:**27484–27491.
52. **MacLennan, D. H., and E. G. Kranias.** 2003. Phospholamban: a crucial regulator of cardiac contractility. Nat. Rev. Mol. Cell Biol. **4:**566–577.
53. **Maekawa, M., T. Ishizaki, S. Boku, N. Watanabe, A. Fujita, A. Iwamatsu, T. Obinata, K. Ohashi, K. Mizuno, and S. Narumiya.** 1999. Signaling from Rho to the actin cytoskeleton through protein kinases ROCK and LIM-kinase. Science **285:**895–898.
54. **Maron, B. J., J. M. Gardin, J. M. Flack, S. S. Gidding, T. T. Kurosaki, and D. E. Bild.** 1995. Prevalence of hypertrophic cardiomyopathy in a general population of young adults. Echocardiographic analysis of 4111 subjects in the CARDIA Study. Coronary Artery Risk Development in (Young) Adults. Circulation **92:**785–789.
55. **Maron, B. J., I. Olivotto, P. Spirito, S. A. Casey, P. Bellone, T. E. Gohman, K. J. Graham, D. A. Burton, and F. Cecchi.** 2000. Epidemiology of hypertrophic cardiomyopathy-related death: revisited in a large non-referral-based patient population. Circulation **102:**858–864.
56. **McCullagh, K. J., C. Juel, M. O'Brien, and A. Bonen.** 1996. Chronic muscle stimulation increases lactate transport in rat skeletal muscle. Mol. Cell Biochem. **156:**51–57.
57. **McGough, A., B. Pope, W. Chiu, and A. Weeds.** 1997. Cofilin changes the twist of F-actin: implications for actin filament dynamics and cellular function. J. Cell Biol. **138:**771–781.
58. **Meberg, P. J., S. Ono, L. S. Minamide, M. Takahashi, and J. R. Bamburg.** 1998. Actin depolymerizing factor and cofilin phosphorylation dynamics: response to signals that regulate neurite extension. Cell Motil. Cytoskeleton **39:**172–190.
59. **Milner, D. J., G. Weitzer, D. Tran, A. Bradley, and Y. Capetanaki.** 1996. Disruption of muscle architecture and myocardial degeneration in mice lacking desmin. J. Cell Biol. **134:**1255–1270.
60. **Mohri, K., H. Takano-Ohmuro, H. Nakashima, K. Hayakawa, T. Endo, K. Hanaoka, and T. Obinata.** 2000. Expression of cofilin isoforms during development of mouse striated muscles. J. Muscle Res. Cell Motil. **21:**49–57.
61. **Morgan, T. E., R. O. Lockerbie, L. S. Minamide, M. D. Browning, and J. R. Bamburg.** 1993. Isolation and characterization of a regulated form of actin depolymerizing factor. J. Cell Biol. **122:**623–633.
62. **Moriyama, K., K. Iida, and I. Yahara.** 1996. Phosphorylation of Ser-3 of cofilin regulates its essential function on actin. Genes Cells **1:**73–86.
63. **Nakashima, K., N. Sato, T. Nakagaki, H. Abe, S. Ono, and T. Obinata.** 2005. Two mouse cofilin isoforms, muscle-type (MCF) and non-muscle type (NMCF), interact with F-actin with different efficiencies. J. Biochem. (Tokyo) **138:**519–526.
64. **Niwa, R., K. Nagata-Ohashi, M. Takeichi, K. Mizuno, and T. Uemura.** 2002. Control of actin reorganization by Slingshot, a family of phosphatases that dephosphorylate ADF/cofilin. Cell **108:**233–246.
65. **Ono, S., N. Minami, H. Abe, and T. Obinata.** 1994. Characterization of a novel cofilin isoform that is predominantly expressed in mammalian skeletal muscle. J. Biol. Chem. **269:**15280–15286.
66. **Pan, J. W., J. R. Hamm, H. P. Hetherington, D. L. Rothman, and R. G. Shulman.** 1991. Correlation of lactate and pH in human skeletal muscle after exercise by 1H NMR. Magn. Reson. Med. **20:**57–65.
67. **Poole-Wilson, P. A., and I. R. Cameron.** 1975. Intracellular pH and K+ of cardiac and skeletal muscle in acidosis and alkalosis. Am. J. Physiol. **229:**1305–1310.
68. **Pope, B. J., K. M. Zierler-Gould, R. Kuhne, A. G. Weeds, and L. J. Ball.** 2004. Solution structure of human cofilin: actin binding, pH sensitivity, and relationship to actin-depolymerizing factor. J. Biol. Chem. **279:**4840–4848.
69. **Postel, R., P. Vakeel, J. Topczewski, R. Knoll, and J. Bakkers.** 2008. Zebrafish integrin-linked kinase is required in skeletal muscles for strengthening the integrin-ECM adhesion complex. Dev. Biol. **318:**92–101.
70. **Sahlin, K., R. C. Harris, B. Nylind, and E. Hultman.** 1976. Lactate content and pH in muscle obtained after dynamic exercise. Pflugers Arch. **367:**143–149.
71. **Sanoudou, D., and A. H. Beggs.** 2001. Clinical and genetic heterogeneity in nemaline myopathy—a disease of skeletal muscle thin filaments. Trends Mol. Med. **7:**362–368.
72. **Sanoudou, D., M. A. Corbett, M. Han, M. Ghoddusi, M. A. Nguyen, N. Vlahovich, E. C. Hardeman, and A. H. Beggs.** 2006. Skeletal muscle repair in a mouse model of nemaline myopathy. Hum. Mol. Genet. **15:**2603–2612.
73. **Stronach, B. E., P. J. Renfranz, B. Lilly, and M. C. Beckerle.** 1999. Muscle LIM proteins are associated with muscle sarcomeres and require dMEF2 for their expression during Drosophila myogenesis. Mol. Biol. Cell **10:**2329–2342.
74. **Sumi, T., K. Matsumoto, Y. Takai, and T. Nakamura.** 1999. Cofilin phosphorylation and actin cytoskeletal dynamics regulated by rho- and Cdc42-activated LIM-kinase 2. J. Cell Biol. **147:**1519–1532.
75. **Taylor, D. J., G. J. Kemp, C. G. Woods, J. H. Edwards, and G. K. Radda.** 1993. Skeletal muscle bioenergetics in myotonic dystrophy. J. Neurol. Sci. **116:**193–200.
76. **Thom, T., N. Haase, W. Rosamond, V. J. Howard, J. Rumsfeld, T. Manolio, Z. J. Zheng, K. Flegal, C. O'Donnell, S. Kittner, D. Lloyd-Jones, D. C. Goff, Jr., Y. Hong, R. Adams, G. Friday, K. Furie, P. Gorelick, B. Kissela, J. Marler, J. Meigs, V. Roger, S. Sidney, P. Sorlie, J. Steinberger, S. Wasserthiel-Smoller, M. Wilson, and P. Wolf.** 2006. Heart disease and stroke statistics—2006 update: a report from the American Heart Association Statistics Committee and Stroke Statistics Subcommittee. Circulation **113:**e85–e151.
77. **Toshima, J., J. Y. Toshima, T. Amano, N. Yang, S. Narumiya, and K.**

Mizuno. 2001. Cofilin phosphorylation by protein kinase testicular protein kinase 1 and its role in integrin-mediated actin reorganization and focal adhesion formation. Mol. Biol. Cell **12:**1131–1145.
78. **Toshima, J., J. Y. Toshima, K. Takeuchi, R. Mori, and K. Mizuno.** 2001. Cofilin phosphorylation and actin reorganization activities of testicular protein kinase 2 and its predominant expression in testicular Sertoli cells. J. Biol. Chem. **276:**31449–31458.
79. **Tran, T. C., C. Singleton, T. S. Fraley, and J. A. Greenwood.** 2005. Cysteine-rich protein 1 (CRP1) regulates actin filament bundling. BMC Cell Biol. **6:**45.
80. **Vartiainen, M. K., T. Mustonen, P. K. Mattila, P. J. Ojala, I. Thesleff, J. Partanen, and P. Lappalainen.** 2002. The three mouse actin-depolymerizing factor/cofilins evolved to fulfill cell-type-specific requirements for actin dynamics. Mol. Biol. Cell **13:**183–194.
81. **von der Hagen, M., S. H. Laval, L. M. Cree, F. Haldane, M. Pocock, I. Wappler, H. Peters, H. A. Reitsamer, H. Hoger, M. Wiedner, F. Oberndorfer, L. V. Anderson, V. Straub, R. E. Bittner, and K. M. Bushby.** 2005. The differential gene expression profiles of proximal and distal muscle groups are altered in pre-pathological dysferlin-deficient mice. Neuromuscul. Disord. **15:**863–877.
82. **Wilding, J. R., J. E. Schneider, A. E. Sang, K. E. Davies, S. Neubauer, and K. Clarke.** 2005. Dystrophin- and MLP-deficient mouse hearts: marked differences in morphology and function, but similar accumulation of cytoskeletal proteins. FASEB J. **19:**79–81.
83. **Winokur, S. T., Y. W. Chen, P. S. Masny, J. H. Martin, J. T. Ehmsen, S. J. Tapscott, S. M. van der Maarel, Y. Hayashi, and K. M. Flanigan.** 2003. Expression profiling of FSHD muscle supports a defect in specific stages of myogenic differentiation. Hum. Mol. Genet. **12:**2895–2907.
84. **Witt, C. C., Y. Ono, E. Puschmann, M. McNabb, Y. Wu, M. Gotthardt, S. H. Witt, M. Haak, D. Labeit, C. C. Gregorio, H. Sorimachi, H. Granzier, and S. Labeit.** 2004. Induction and myofibrillar targeting of CARP, and suppression of the Nkx2.5 pathway in the MDM mouse with impaired titin-based signaling. J. Mol. Biol. **336:**145–154.
85. **Yang, N., O. Higuchi, K. Ohashi, K. Nagata, A. Wada, K. Kangawa, E. Nishida, and K. Mizuno.** 1998. Cofilin phosphorylation by LIM-kinase 1 and its role in Rac-mediated actin reorganization. Nature **393:**809–812.
86. **Yeoh, S., B. Pope, H. G. Mannherz, and A. Weeds.** 2002. Determining the differences in actin binding by human ADF and cofilin. J. Mol. Biol. **315:** 911–925.
87. **Yonezawa, N., E. Nishida, and H. Sakai.** 1985. pH control of actin polymerization by cofilin. J. Biol. Chem. **260:**14410–14412.
88. **Zhan, Q., J. R. Bamburg, and J. A. Badwey.** 2003. Products of phosphoinositide specific phospholipase C can trigger dephosphorylation of cofilin in chemoattractant stimulated neutrophils. Cell Motil. Cytoskeleton **54:**1–15.
89. **Zolk, O., P. Caroni, and M. Bohm.** 2000. Decreased expression of the cardiac LIM domain protein MLP in chronic human heart failure. Circulation **101:** 2674–2677.